Check for updates

Received: 27 November 2021 | Revised: 14 January 2022 | Accepted: 30 January 2022

DOI: 10.1002/apj.2754

RESEARCH ARTICLE

Asia-Pacific Journal of Chemical Engineering | Curtin University | WILEY

Experimental study of metal-oxide nanoparticles on the thermal properties of erythritol for thermal energy storage

Hao Zhou | **Laiquan Lv** | **Mengting Ji** | **Yize Zhang** | **Fangzheng Cheng** | **Kefa Cen**

State Key Laboratory of Clean Energy Utilization, Institute for Thermal Power Engineering, Zhejiang University, Hangzhou, PR China

Correspondence
Hao Zhou, State Key Laboratory of Clean Energy Utilization, Institute for Thermal Power Engineering, Zhejiang University, Hangzhou 310027, PR China.
Email: zhouhao@zju.edu.cn

Funding information
National Natural Science Foundation of China, Grant/Award Number: 52036008

Abstract

Erythritol has attracted wide attention due to high latent heat of 297.2 kJ/kg and excellent chemical stability as a medium- to low-temperature thermal energy storage (TES) material. However, low thermal conductivity leads to extended charging and discharging time and severely affects its large-scale application. In this article, three cheap nanoparticles (CuO, Al_2O_3, and Fe_2O_3) and triethanolamine (TEA) were used as heat transfer enhancers and dispersant to improve the TES performance of erythritol. Sedimentation of nanoparticles in erythritol indicates that TEA is an effective dispersant in erythritol for three kinds of nanoparticles. The experimental results show that the thermal conductivity increased from 0.671 W/(m·K) of erythritol to 0.722 W/(m·K) and 0.761 W/(m·K) of 1.5 wt% CuO and Fe_2O_3 nano-enhanced phase change materials (NePCMs), respectively. Based on the DSC results, the melting temperature and heat of fusion of NePCMs stayed stable with nanoparticles but increased significantly after adding TEA. Furthermore, the charging/discharging cyclic behaviors of NePCMs were tested in the cycle test platform. During the cycle test, the melting time of 1.5 wt% CuO NePCM decreased from 657.9 s for pure erythritol to 615.8 s but increased to 757 s and 680.6 s for 1.5 wt% Al_2O_3 and 1.5 wt% Fe_2O_3 NePCMs. The solidification time decreased from 311.2 s for erythritol to 179.3 s, 198.5 s, and 132.4 s for 1.5 wt% CuO, 1.5 wt% Al_2O_3, and 1.5 wt% Fe_2O_3 NePCMs. Interestingly, the supercooling degree of NePCMs we got from the test was much lower than that from the DSC curves, indicating that the supercooling is related to the sample size. These results testify that CuO and Fe_2O_3 nanoparticles can improve the thermal conductivity of erythritol effectively.

KEYWORDS

composite-phase change materials, metal-oxide nanoparticles, supercooling degree, thermal conductivity, thermal energy storage

1 | INTRODUCTION

Energy sources such as fossil fuels can be used to provide energy according to the demand of people, which means they are readily storable when not needed. However, renewable energy like solar and wind energy needs to be harvested when available and stored until required.[1,2] Thermal energy storage (TES) is an appropriate solution

 © 2022 Curtin University and John Wiley & Sons, Ltd.

19322143, 2022, 2, Downloaded from https://onlinelibrary.wiley.com/doi/10.1002/apj.2754 by Zhejiang University, Wiley Online Library on [12/02/2023]. See the Terms and Conditions (https://onlinelibrary.wiley.com/terms-and-conditions) on Wiley Online Library for rules of use; OA articles are governed by the applicable Creative Commons License

to solve the unbalance between energy demand and supply.[3,4] Generally, TES can be commonly achieved as sensible heat storage,[5–7] latent heat storage (LHS),[8–10] and thermochemical storage[11–13] based on the way thermal energy is stored.

LHS has many advantages in energy density and technological maturity that are not available in sensible heat storage and thermochemical storage.[14] LHS can realize heat storage and release almost without temperature variation, whose gravimetric energy density is 2–4 times[12] higher than sensible heat storage.[15] Besides, LHS has a smaller volume of the TES system and less heat loss during the process of heat storage.

Phase change materials (PCMs) are employed to absorb and release heat through the phase change process of PCMs in LHS. PCMs are categorized based on their phase change temperature as low-, medium-, and high-temperature PCMs.[10] According to the report of Hoshi et al.,[16] the melting temperature of PCMs below 227°C can be classified into the low-temperature category, those with melting temperature between 227°C and 427°C as medium-temperature PCMs, and those with melting temperature over 427°C as high-temperature PCMs. Organic low-temperature PCMs such as paraffins, fatty acids, esters, and alcohols receive wide attention due to their great chemical stability, recyclability, high latent heat, and uniform melting ability.[10] Erythritol, with a melting temperature of 116°C, has higher energy storage density and satisfactory supercooling. Moreover, erythritol is nontoxic, noncorrosive, and environmentally friendly, making it a promising PCM candidate.[17] However, the low thermal conductivity leads to long charging and discharging time of erythritol, restricting its application seriously. Qureshi et al.,[18] Wei et al.,[15] and Wu et al.[8] reviewed recent enhancement researches on thermal conductivity of PCMs.

In view of the poor thermal conductivity of PCMs, scholars put forward numerous ways to overwhelm the problem, such as adding high thermal conductivity nanoparticles,[19,20] metallic foams,[21–23] expanded graphite,[24,25] and other materials[26,27] into PCMs. The nano-enhanced PCMs (NePCMs) were proposed by Khodadadi and Hosseinizadeh[28] to improve the thermal conductivity of PCMs by adding nanoparticles to them. Subsequently, different kinds of nanoparticles were used to enhance the thermal properties of PCMs, and the mechanisms of enhanced heat transfer of nanoparticles were investigated intensively.[29,30] Rashidi et al.[31] reviewed the features such as the thermal conductivity, specific heat, and dynamic viscosity of the nanofluids with hybrid nanostructures and the proposed models for these properties.

A paraffin/diatomite composite PCM was prepared by Xu and Li,[32] in which 0.26 wt% of multiwall carbon nanotubes with length ranging 5–15 μm and diameter 10–20 nm were added. The thermal conductivity of the paraffin/diatomite composite PCM increased by 42.45%. At the same time, multiwall carbon nanotubes accelerated the heat storage and release rates obviously. Srinivasan et al.[33] found that the thermal conductivity of eicosane-based composite PCM was enhanced to 4.5 times of eicosane by dispersing 3.5 vol% graphite particles into it. Zhang et al.[34] investigated the effect of short carbon fibers on the thermal properties of pure erythritol. The thermal conductivity was enhanced from 0.77 W/(m·K) of pure erythritol to 3.92 W/(m·K) by adding 10 wt% short carbon fibers into erythritol.

Ghossein et al.[35] prepared NePCMs with different mass fractions by suspending silver nanoparticles into eicosane. The thermal conductivity increased from 0.42 W/(m·K) of eicosane to 0.48 W/(m·K) of NePCMs with 2 wt% Ag nanoparticles. Parameshwaran et al.[36] used silver–titania hybrid nanocomposite to improve the thermal conductivity of organic dibasic ester. The thermal conductivity of organic dibasic ester was 0.386 W/(m·K), while increased to 0.860 W/(m·K) after adding 1.0 wt% hybrid nanocomposite. Suresh Kumar et al.[37] reported that the thermal conductivity of capric acid increased from 0.150 W/(m·K) to 0.397 W/(m·K) by dispersing 0.8 wt% CuO nanoparticles into it. Colla et al.[38] obtained NePCMs by seeding 1 wt% of nano-aluminum oxide and carbon black in paraffin. The characterization results showed that the carbon black nanoparticles increased the thermal conductivity from 0.254 W/(m·K) of paraffin to 0.344 W/(m·K), while the Al_2O_3 nanoparticles abated it. The dispersion technique was applied by Şahan et al.[39] to improve the heat transfer of paraffin by adding nano-magnetite into it. The LHS capacity of the composite PCM was 3% and 8% higher than pure paraffin, and the thermal conductivity was improved by 48% and 60% after adding nano-magnetite content of 10 wt% and 20 wt%, respectively. Table 1 lists the thermal conductivity of organic PCMs before and after adding different kinds of nanoparticles. Recently, NePCMs have been employed in different fields of science and industrial applications, such as incorporating nanomaterials into PCM for solar TES[46] and heat exchangers. The application research of large-scale NePCMs becomes more and more important.[47]

Admittedly, there are some researches about adding nanoparticles into PCMs to improve the thermal conductivity of PCMs, but the investigations mainly focus on the thermal properties changes of PCM after adding nanoparticles and the cyclic stability of small mass NePCM. Few works consider both the effects of different

19322143, 2022, 2, Downloaded from https://onlinelibrary.wiley.com/doi/10.1002/apj.2754 by Zhejiang University, Wiley Online Library on [12/02/2023]. See the Terms and Conditions (https://onlinelibrary.wiley.com/terms-and-conditions) on Wiley Online Library for rules of use; OA articles are governed by the applicable Creative Commons License

TABLE 1 Thermal conductivity of organic PCMs before and after adding different kinds of nanoparticles

Organic PCMs	Nanoparticles	Thermal conductivity of PCMs (W/(m·K))	Content (%)	Thermal conductivity of NePCMs (W/(m·K))	Magnification (times)	Refs
Eicosane	Ag	0.42	2	0.48	1.143	[35]
Organic ester	Ag	0.257	5	0.765	2.977	[36]
Organic dibasic ester	Ag–TiO_2	0.386	1	0.860	2.402	[40,41]
Lauric acid/ stearic acid	TiO_2	0.198	1	0.267	1.348	[42]
	ZnO		1	0.291	1.470	[42]
	CuO		1	0.321	1.621	[42]
Rubitherm RT42	CuO	0.2000	0.5	0.2007	1.0035	[43]
Capric acid	CuO	0.150	0.8	0.397	2.647	[37]
Sodium acetate trihydrate	Cu	0.777	0.5	0.936	1.205	[44]
RT20	Al_2O_3	0.254	1	0.234	0.921	[38]
RT25	Al_2O_3	0.260	1	0.242	0.931	[38]
Pentaerythritol	Al_2O_3	0.106	0.1, 0.5, 1	0.1252, 0.1412, 0.1609	1.181, 1.332, 1.518	[45]
Paraffin	Fe_3O_4	0.25	10	0.37	1.48	[39]

nanoparticles on the thermal properties of PCM and the charging and discharging cyclic behaviors of NePCM with a large mass. In this article, three cheap and frequently used nanoparticles (CuO, Al_2O_3, and Fe_2O_3) were chosen as heat transfer enhancers to improve the thermal conductivity of erythritol. However, directly mixing nanoparticles with PCM may cause nanoparticles to sediment at the bottom of liquid PCM, resulting in invalid of nanoparticles. Therefore, adding effective dispersant can meet the particular requirements of NePCMs, such as even suspension, stable and durable suspension, and low agglomeration of particles. According to the research of Zhichao et al.,[20] triethanolamine (TEA) was an efficient dispersant to prevent nanoparticles deposition in erythritol. Hence, erythritol and TEA were used as based PCM and dispersant, respectively. Nine kinds of NePCMs with different nanoparticles and the mass content of 0.5%, 1%, and 1.5% were prepared and characterized systematically. To be more specific, the microstructure of nanoparticles (transmission electron microscope [TEM]), chemical compatibility (X-ray powder diffractometer [XRD]), thermal properties (differential scanning calorimeter [DSC]), and thermal conductivity (thermal constant analyzer) of the NePCMs were studied. At last, the charging/discharging cyclic behaviors of NePCMs were investigated experimentally based on the cyclic test platform. The results of this study can provide some valuable information for the application of nanoparticles as heat transfer enhancers in TES and make the application of NePCMs in solar energy storage systems, thermal management of building, and electronic components.

2 | MATERIALS AND METHODS

2.1 | Materials and preparation

Erythritol (purity: 99%) and TEA (purity ≥99) were provided by Shanghai Macklin Biochemical Technology Co. Ltd. and Aladdin Chemistry Co. Ltd. of China, respectively. The main information and the morphology (FEI, Tecnai G2 F20, USA) of three selected nanoparticles are listed in Table 2 and displayed in Figure 1.

The typical two-step method[20,48] was employed to prepare the NePCMs. Firstly, erythritol was weighted with a balance and completely melted to a clear liquid in an oil bath (HH-51BS/300°C/±0.5°C) at 130°C. After that, TEA, whose mass content was half of the nanoparticles, was added and stirred for 30 min in a magnetic stirring apparatus to fully mix the dispersant and

19322143, 2022, 2, Downloaded from https://onlinelibrary.wiley.com/doi/10.1002/apj.2754 by Zhejiang University, Wiley Online Library on [12/02/2023]. See the Terms and Conditions (https://onlinelibrary.wiley.com/terms-and-conditions) on Wiley Online Library for rules of use; OA articles are governed by the applicable Creative Commons License

TABLE 2 Main information of three kinds of nanoparticles

Nanoparticle type	Supplier	Purity (%)	Nominal diameter (nm)	Density (kg/m^3)
Cupric oxide (CuO)	Macklin	99.5	40	6.32
Aluminum oxide (Al_2O_3)	Macklin	99.9	30	3.97
Ferric oxide (Fe_2O_3)	Aladdin	99.5	30	5.24

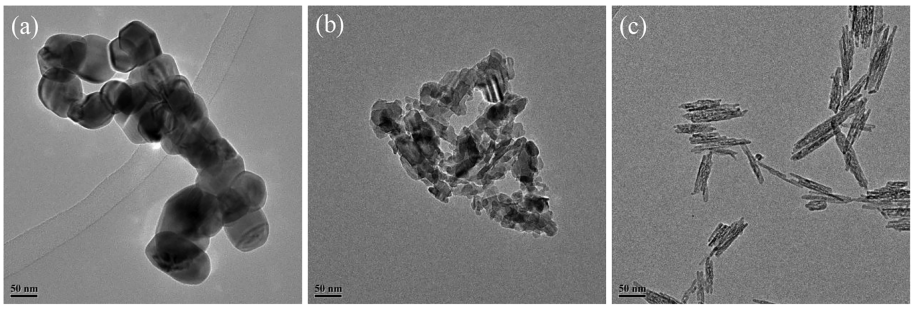

FIGURE 1 Morphology of (a) CuO, (b) Al_2O_3, and (c) Fe_2O_3 nanoparticles in transmission electron microscopy (TEM)

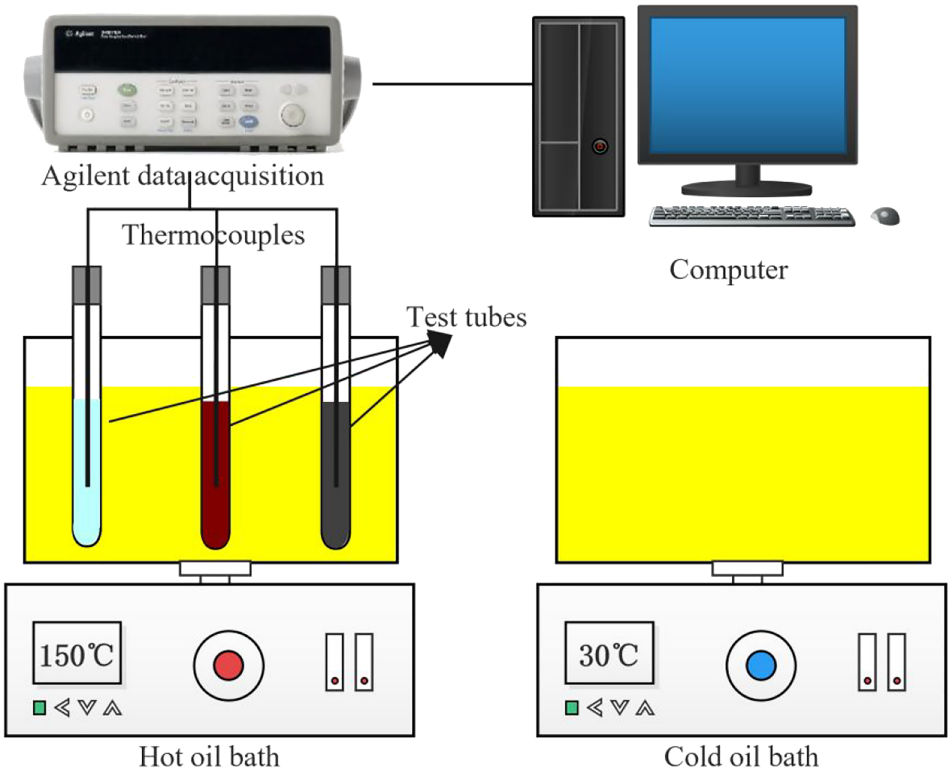

FIGURE 2 Experimental setup for testing the cyclic behaviors of PCMs

liquid erythritol. Then a fixed mass of nanoparticles was added and stirred for 30 min again to get well-mixed NePCMs. Eighteen groups of NePCMs (0.5 wt%, 1 wt%, and 1.5 wt% CuO, Al_2O_3, and Fe_2O_3 with and without TEA) were prepared. Finally, the NePCMs were poured into some molds with a diameter of 50 mm for rapid cooling, and the thermal conductivity test was performed after they were solidified and polished carefully. Each sample was prepared more than four times during the experiment to minimize experimental error.

2.2 | Characterization

An X-ray diffractometer (X'Pert Powder, the Netherlands) with Cu K-alpha radiation ($k = 1.540598$ Å) from 10° to 90° was employed to characterize the crystal size of erythritol, nanoparticles, and NePCMs. The scanning rate and step size were 0.1°/min and 0.02°. The thermal conductivity of NePCMs was characterized by a thermal constant analyzer (TPS 2500S, Hot Disk Co., Ltd., Sweden, accuracy: ±0.0001 W/(m·K)) based on the

19322143, 2022, 2, Downloaded from https://onlinelibrary.wiley.com/doi/10.1002/apj.2754 by Zhejiang University, Wiley Online Library on [12/02/2023]. See the Terms and Conditions (https://onlinelibrary.wiley.com/terms-and-conditions) on Wiley Online Library for rules of use; OA articles are governed by the applicable Creative Commons License

transient planar heat source method at room temperature of 23 ± 0.5°C. To avoid the experimental error caused by the sample as much as possible, we took the sample out of the mold and carefully polished the ground of the sample. During the test, a 5501 probe inserted between the two polished surfaces was employed as a heat source and a sensor to measure the thermal conductivity of the samples every 25 min. The result that was significantly different from the average value obtained by the test would be eliminated. In addition, the mean value obtained from the test without abnormal results was applied as the thermal conductivity result.

The melting temperature, solidification temperature, and latent heat of erythritol and the NePCMs were measured by the DSC (Q200, TA, USA, accuracy: ±0.05°C) with a constant stream of nitrogen whose flow rate was 50 mL/min. All the samples with the size of 12–15 mg were heated from room temperature to 160°C at 20°C/min to eliminate the thermal history. During the test, it was found that the NePCMs with TEA did not show an endothermic peak when the temperature was lowered to 30°C. Therefore, we set a lower temperature limit of NePCMs with TEA to −30°C during the cooling process. The samples without TEA were cooled from 160°C to 30°C and then heated from 30°C to 160°C again at 5°C/min, while the samples with TEA were cooled from 160°C to −30°C and then heated from −30°C to 160°C again at 5°C/min. An electron microscope (Axioskop 2 Plus, Zeiss, Germany) was used to photograph the surface microstructure of erythritol and NePCMs.

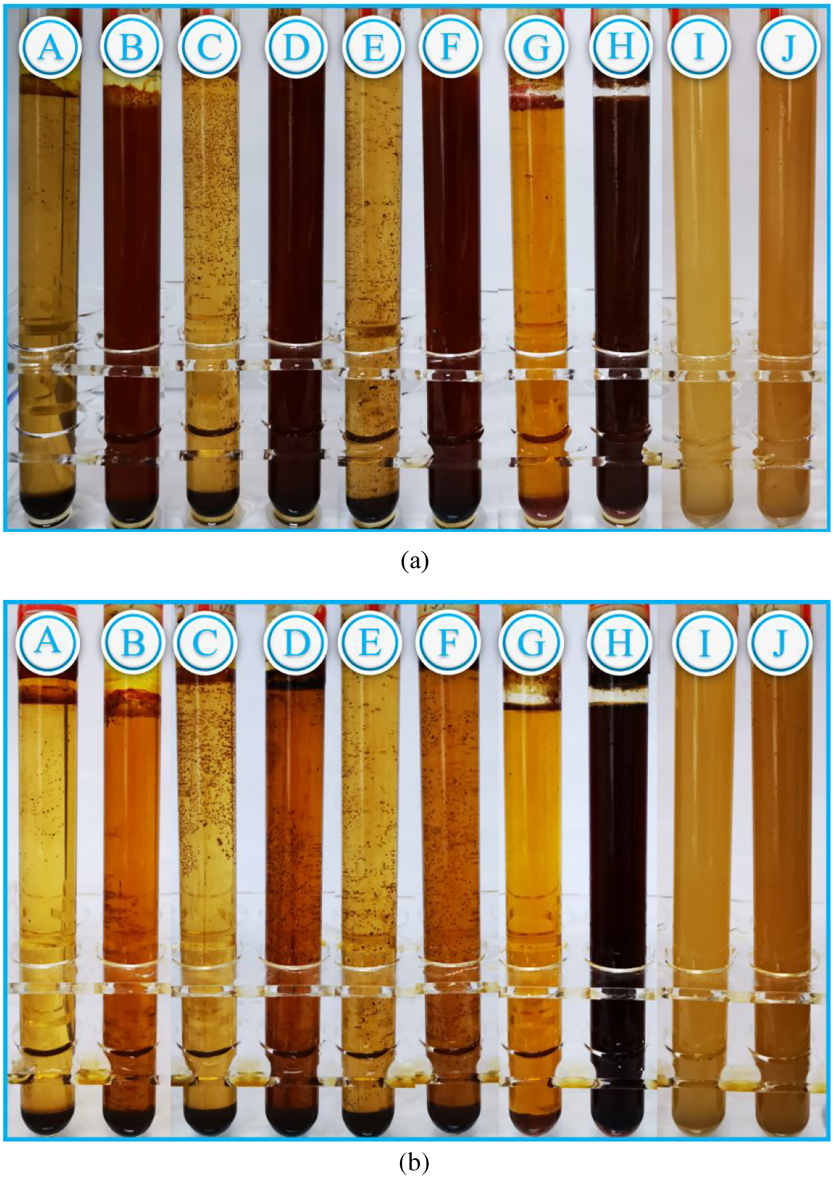

FIGURE 3 Photography of the sedimentation of nanoparticles ([A–F] 0.5 wt%, 1 wt%, and 1.5 wt% Fe_2O_3 NePCMs without and with TEA; [G, H] 1.5 wt% CuO NePCM without and with TEA; and [I, J] 1.5 wt% Al_2O_3 NePCM without and with TEA) in erythritol under 140°C after (a) 48 h and (b) 120 h

19322143, 2022, 2, Downloaded from https://onlinelibrary.wiley.com/doi/10.1002/apj.2754 by Zhejiang University, Wiley Online Library on [12/02/2023]. See the Terms and Conditions (https://onlinelibrary.wiley.com/terms-and-conditions) on Wiley Online Library for rules of use; OA articles are governed by the applicable Creative Commons License

2.3 | Sedimentation of nanoparticles in erythritol and charging/discharging cyclic behaviors of NePCMs

The heat transfer of PCM can be enhanced by introducing nanoparticles into it. However, the difference in density between the two materials will cause the sedimentation of nanoparticles in the PCM and cause the failure of NePCM. In our study, we used TEA as the dispersant of nanoparticles in erythritol. Each NePCM (1.5 wt% CuO and Al_2O_3, 0.5 wt% Fe_2O_3, 1 wt% Fe_2O_3, and 1.5 wt% Fe_2O_3 with and without TEA) with a mass of 20 g was photographed every 24 h in an oil bath of 140°C, through which we could obtain sedimentation of nanoparticles in erythritol.

To better investigate the charging and discharging cyclic behaviors of PCMs, a test platform of cyclic behavior was set up, as displayed in Figure 2. The test platform contained a hot oil bath (150°C), a cold oil bath (30°C), test tubes, a temperature measuring system (Agilent data acquisition, K-type thermocouples/±1°C), and a computer, which collected data every 2 s. Six test tubes whose diameter and height were 25 mm and 150 mm were placed in the holder to conduct the cycle test. Add 50 g PCM to each test tube with a silicone plug above it, and a thermocouple was inserted in the center of the tube to monitor the temperature change of PCM. The test tubes were heated and cooled alternately in the hot and cold oil bath during the test. The data obtained from the measuring system could monitor the phase change processes of PCMs.

3 | RESULTS AND DISCUSSION

3.1 | Sedimentation of nanoparticles in erythritol

The sedimentation of different kinds of nanoparticles in erythritol in an oil bath of 140°C after 48 h and 120 h is displayed in Figure 3. As revealed in Figure 3a, all kinds of nanoparticles in the NePCMs without TEA showed noticeable sedimentation after 48 h. However, only a tiny number of Fe_2O_3 particles sedimented in the Fe_2O_3 NePCMs with TEA, while no visible sedimentation of nanoparticles was found in the other two NePCMs with TEA. The sedimentation of nanoparticles became more severe in the NePCMs without TEA after 120 h, as shown in Figure 3b. There were more Fe_2O_3 nanoparticles sedimented in the NePCMs with TEA. Correspondingly, no distinct layer was observed in the CuO and Al_2O_3 NePCMs. It can be concluded from Figure 3 that TEA is an effective dispersant in erythritol in general. It is noteworthy that TEA is more efficient for the dispersion of CuO and Al_2O_3 nanoparticles in erythritol. This may be explained by the research of Zhichao et al.[20] There are several main reasons: (1) Compared with other dispersants, TEA molecules can form functional nanolayers more easily. (2) Secondly, the protons from alcohol molecules can be taken by TEA easily because of the lone pair electrons on the nitrogen atom.[49] (3) Thirdly, hydrogen bond can be formed between TEA and erythritol molecule due to the hydroxide radical of TEA.

3.2 | XRD analysis of NePCMs

The composition of the material can be obtained through the XRD pattern. The XRD patterns of erythritol, nano-CuO, nano-Al_2O_3, nano-Fe_2O_3, and NePCMs are displayed in Figure 4. Several strong diffraction peaks were observed at 14.6°, 19.5°, 20.1°, 24.5°, and 29.5° in the XRD pattern of erythritol, which was in accordance with the results of Shao et al.[50] and Karthik et al.[51] There were two strong diffraction peaks located at $2\theta = 32.8°$ and 67.5° in the XRD pattern of nano-CuO, which was consistent with standard JCPDS file no. 48-1548. The diffraction intensity of nano-Al_2O_3 and nano-Fe_2O_3 was weaker than the other samples, so the values of the two samples in Figure 4 were magnified 10 times. The XRD patterns of nano-Al_2O_3 and nano-Fe_2O_3 are similar to JCPDS file no. 35-0221 and no. 33-0664. According to Figure 4, the XRD patterns of NePCMs were approximately identical to erythritol, indicating that the addition of nanoparticles produced no crystal change in erythritol.

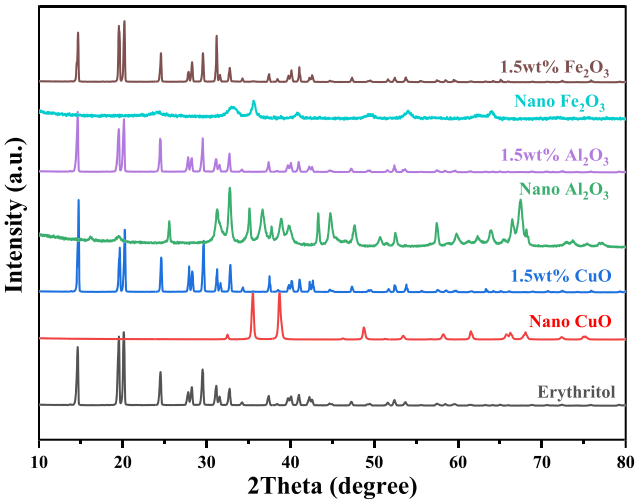

FIGURE 4 XRD patterns of erythritol, nano-CuO, nano-Al_2O_3, nano-Fe_2O_3, and 1.5 wt% CuO, 1.5 wt% Al_2O_3, and 1.5 wt% Fe_2O_3 NePCMs

19322143, 2022, 2, Downloaded from https://onlinelibrary.wiley.com/doi/10.1002/apj.2754 by Zhejiang University, Wiley Online Library on [12/02/2023]. See the Terms and Conditions (https://onlinelibrary.wiley.com/terms-and-conditions) on Wiley Online Library for rules of use; OA articles are governed by the applicable Creative Commons License

3.3 | Thermal conductivity of NePCMs

Thermal conductivity dominates the charging and discharging time of PCM, which is vital for PCM applications. Figure 5 plots the thermal conductivity of pure erythritol and NePCMs having different kinds and contents of nanoparticles with TEA. Consistent with the results of Wang et al.,[26] the thermal conductivity of pure erythritol was 0.671 W/(m·K). As expected, that of NePCMs increased with the increase of CuO and Fe_2O_3 nanoparticles, which indicated that the two kinds of nanoparticles could efficiently improve the heat transfer of erythritol. The thermal conductivity of 1.5 wt% CuO and Fe_2O_3 NePCMs was enhanced to 0.722 W/(m·K) and 0.761 W/(m·K), respectively. More interestingly, the Al_2O_3 nanoparticles improved the thermal conductivity of erythritol at 0.5 wt% and 1.5 wt% but weakened it at 1 wt%. Similar results were reported in Colla et al.[38] The influence factors of Al_2O_3 nanoparticles on the thermal conductivity of PCM need further research. Especially, Figure 5 plots the thermal conductivity fitting curves of CuO and Fe_2O_3 NePCMs.

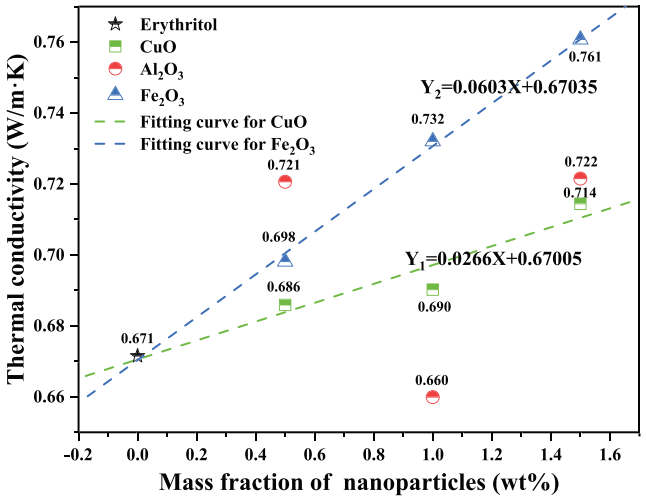

FIGURE 5 Thermal conductivity of erythritol, CuO, Al_2O_3, and Fe_2O_3 NePCMs and fitting curves for CuO and Fe_2O_3 NePCMs

The surface microstructure of erythritol and NePCMs having different kinds and contents of nanoparticles with TEA is presented in Figure 6. Compared with the surface microstructure of erythritol, the surfaces of NePCMs with TEA were rougher and more cracks appeared. As revealed in Figure 6d–f, with the increase of Fe_2O_3 nanoparticles, the cracks on the surface became denser and changed from strips to dendrites. The possible reason is that the nucleation center will increase by introducing nanoparticles into erythritol. Simultaneously, the thermal conductivity of erythritol will improve, which will promote the rapid growth of grains.

3.4 | DSC analysis of NePCMs

The thermophysical properties of PCM can affect the TES performance of PCM significantly. The DSC curves during the heating and cooling processes of PCMS are revealed in Figure 7. The phase transition temperature of PCM is the peak of heating and cooling curves, while the latent heat is obtained by integrating the area enclosed by the baseline and the peak of the curve. The detailed information about thermophysical properties of erythritol and NePCMs is listed in Table 3.

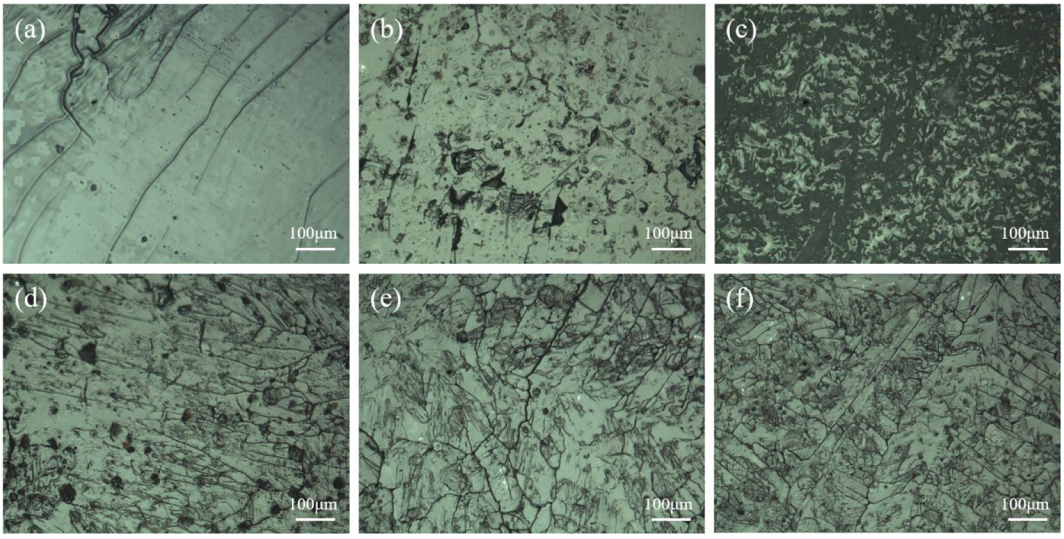

FIGURE 6 Surface microstructure of (a) erythritol, (b) 1.5 wt% CuO, (c) 1.5 wt% Al_2O_3, (d) 0.5 wt% Fe_2O_3, (e) 1 wt% Fe_2O_3, and (f) 1.5 wt% Fe_2O_3 NePCMs

19322143, 2022, 2, Downloaded from https://onlinelibrary.wiley.com/doi/10.1002/apj.2754 by Zhejiang University, Wiley Online Library on [12/02/2023]. See the Terms and Conditions (https://onlinelibrary.wiley.com/terms-and-conditions) on Wiley Online Library for rules of use; OA articles are governed by the applicable Creative Commons License

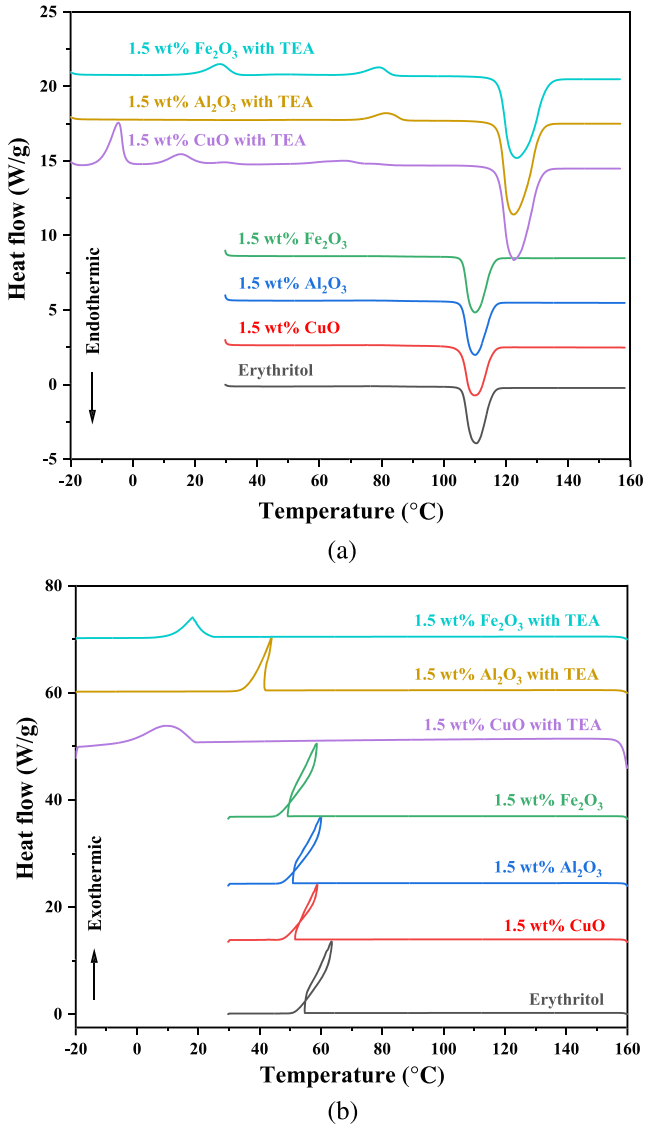

FIGURE 7 DSC curves of erythritol, 1.5 wt% CuO, 1.5 wt% Al_2O_3, 1.5 wt% Fe_2O_3, 1.5 wt% CuO with TEA, 1.5 wt% Al_2O_3 with TEA, and 1.5 wt% Fe_2O_3 with TEA for (a) melting and (b) solidification processes

As shown in Figure 7 and Table 3, the addition of nanoparticles had almost no effect on the melting temperature of NePCMs, but the solidification temperature of NePCMs had decreased to varying degrees, which would lead to the increase of supercooling degree. After adding 1.5 wt% CuO, Al_2O_3, and Fe_2O_3 nanoparticles into erythritol, the supercooling degree of NePCMs increased from 47.03°C of erythritol to 51.26°C, 50.16°C, and 51.41°C, respectively. For latent heat of NePCMs, the phase transition temperature of nanoparticles was much higher than erythritol, which indicated that no phase transition occurred for nanoparticles during the DSC test. Therefore, in contrast with pure erythritol, the heat of fusion and solidification of NePCMs added with nanoparticles were reduced proportionally.[14,52] The experimental results from DSC curves were similar to the theoretical results.

One unanticipated finding was that after adding the dispersant TEA on the basis of adding nanoparticles to erythritol, the melting temperature and heat of fusion of all NePCMs increased significantly. The melting temperature of NePCMs with TEA added three nanoparticles increased from 110.09°C, 110.09°C, and 109.99°C to 122.52°C, 122.38°C, and 123.48°C, respectively, while the heat of fusion increased from 288.9 kJ/kg, 292.8 kJ/kg, and 292.7 kJ/kg to 347.8 kJ/kg, 343.8 kJ/kg, and 347.6 kJ/kg. The conceivable reasons for this phenomenon were described in Section 3.1 that hydrogen bond between TEA and erythritol molecule can be formed easily due to the hydroxide radical of TEA. Compared with substances without hydrogen bonds between molecules, substances with hydrogen bonds need higher temperature when melting to provide more energy to break the hydrogen bonds between molecules. Consequently, the melting temperature and heat of fusion of substances with hydrogen bonds are higher than those without hydrogen bonds. In addition, we observed that the NePCMs with TEA showed an exothermic peak during the cooling process, and several other exothermic peaks appeared during the following heating process, which was related to the addition of TEA. In Section 3.5, we will discuss the charging and discharging behaviors of PCMs in more detail.

3.5 | Charging and discharging cyclic behaviors of NePCMs

The charging and discharging behaviors of erythritol, 1.5 wt% CuO, Al_2O_3, and Fe_2O_3, 1 wt% Fe_2O_3, and 0.5 wt % Fe_2O_3 NePCMs with TEA were researched on the test platform. Consecutive charging and discharging test with 24 cycles was carried out on erythritol and different kinds of NePCMs. Figure 8 displays the typical temperature curve of erythritol with time during a charging/discharging cycle. During the charging process, the temperature increased rapidly until it almost reached the melting temperature (T_m) of erythritol. The temperature then slowly rose to the turning temperature (T_t) due to a large amount of heat absorbed by the melting of erythritol. After the erythritol melted completely, the temperature rose quickly again until it approached the temperature of the heat source. During the discharging process of erythritol, the temperature quickly declined to the solidification temperature (T_s) that was under the melting temperature of erythritol, indicating a supercooling. Subsequently, the erythritol began to solidify accompanied by heat release, and the

19322143, 2022, 2, Downloaded from https://onlinelibrary.wiley.com/doi/10.1002/apj.2754 by Zhejiang University, Wiley Online Library on [12/02/2023]. See the Terms and Conditions (https://onlinelibrary.wiley.com/terms-and-conditions) on Wiley Online Library for rules of use; OA articles are governed by the applicable Creative Commons License

TABLE 3 The melting temperature, solidification temperature, heat of fusion, heat of solidification, and supercooling degree of NePCMs having different kinds of nanoparticles with and without TEA

Samples	Melting temperature (°C)	Solidification temperature (°C)	Heat of fusion (kJ/kg)	Heat of solidification (kJ/kg)	Supercooling degree (°C)
Erythritol	110.47	63.44	297.2	237.4	47.03
1.5 wt% CuO	110.09	58.83	288.9	226.1	51.26
1.5 wt% CuO with TEA	122.52	—	347.8	—	—
1.5 wt% Al_2O_3	110.09	59.93	292.8	229.9	50.16
1.5 wt% Al_2O_3 with TEA	122.38	—	343.8	—	—
1.5 wt% Fe_2O_3	109.99	58.58	292.7	233.3	51.41
1.5 wt% Fe_2O_3 with TEA	123.48	—	347.6	—	—

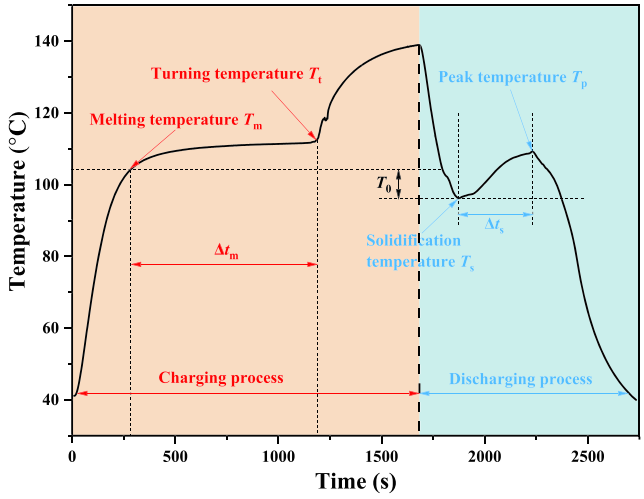

FIGURE 8 Typical temperature curve with time during a charging–discharging cycle for pure erythritol

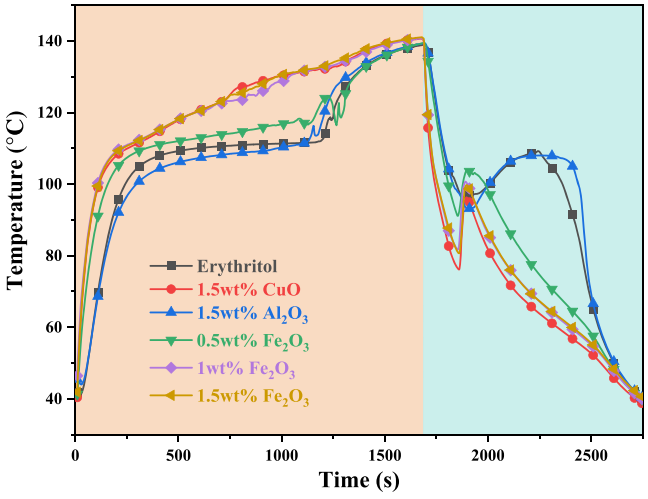

FIGURE 9 The first charging–discharging cycle curves of erythritol, 1.5 wt% CuO, Al_2O_3, and Fe_2O_3, 1 wt% Fe_2O_3, and 1.5 wt % Fe_2O_3 NePCMs with TEA

temperature rose to a particular value and then declined continually.[17]

To better quantify the cyclic behaviors of erythritol and NePCMs, we introduced the following parameters, as plotted in Figure 8. Δt_m was a representative charging time that was the time it took from the melting temperature to the turning temperature. Similarly, Δt_s was the time it took from the solidification temperature to peak temperature (T_p), which represented the discharging time of NePCMs to a certain extent. $T_0 = T_m - T_s$ represented the supercooling degree of NePCMs, as shown in Figure 8.

The first charging/charging cycle curves of erythritol, 1.5 wt% CuO, 1.5 wt% Al_2O_3, 0.5 wt% Fe_2O_3, 1 wt% Fe_2O_3, and 1.5 wt% Fe_2O_3 NePCMs with TEA are revealed in Figure 9. At the beginning of the charging process, the temperature of the five samples was the same. Then it was found that the higher the thermal conductivity, the steeper is the slope of the melting curve. During the discharging process, the extent of shortening the discharging time of high thermal conductivity was more evident than the charging time. Compared with pure erythritol, the discharging time of the NePCMs with CuO and Fe_2O_3 nanoparticles could be shortened evidently. The Δt_s of pure erythritol was 356 s, while that of 1.5 wt% CuO and 1.5 wt% Fe_2O_3 NePCMs was 40 s and 38 s, respectively.

Based on the 24 charging/discharging cycle test, the stability and values of Δt_m, Δt_s, and T_0 were analyzed, as shown in Figure 10. As plotted in Figure 10a–c, the value of Δt_m remained relatively constant during the 24 cycle test, while the values of Δt_s and T_0 were unstable at the

19322143, 2022, 2, Downloaded from https://onlinelibrary.wiley.com/doi/10.1002/apj.2754 by Zhejiang University, Wiley Online Library on [12/02/2023]. See the Terms and Conditions (https://onlinelibrary.wiley.com/terms-and-conditions) on Wiley Online Library for rules of use; OA articles are governed by the applicable Creative Commons License

beginning of the test but then remained relatively stable. This indicates that the performance of erythritol and NePCMs was stabilized during the 24 cycle test.

The box charts of Δt_m, Δt_s, and T_0 during the 24 charging/discharging cycles for erythritol and different NePCMs are displayed in Figure 10d–f. The box chart was invented in 1977 by the famous statistician John Tukey, which can show the maximum, minimum, median, upper, and lower quartiles of a set of data. Moreover, the mean value can represent the compromised state of a data group, and the box height (interquartile range) can reflect the degree of dispersion of the data group.[17,53] Compared with the mean Δt_m of 657.92 s for erythritol, it was decreased by 6.4% and 7.4% for 1.5 wt% CuO and 0.5 wt% Fe_2O_3 NePCMs, while it is increased by 15.1%, 7.6%, and 3.4% for 1.5 wt% Al_2O_3, 1 wt% Fe_2O_3, and 1.5 wt% Fe_2O_3 NePCMs, as shown in Figure 10d.

In contrast with the representative charging time, as revealed in Figure 10e, the representative discharging time difference is more obvious between the erythritol and NePCMs. Compared with the Δt_s of 311.25 s for erythritol, it was decreased by 42.4%, 36.2%, 68.7%, 52.1%, and 57.5% for 1.5 wt% CuO, 1.5 wt% Al_2O_3, 0.5 wt% Fe_2O_3, 1 wt% Fe_2O_3, and 1.5 wt% Fe_2O_3 NePCMs, respectively. Among them, the NePCM with 0.5 wt% Fe_2O_3 had the shortest discharging time. The possible reasons were mentioned in Sections 3.3 and 3.4; as the contents of nanoparticles increase, the thermal conductivity of NePCMs will increase, reducing the solidification time of NePCMs. However, at the same time, the quality of TEA also increases, which will form more hydrogen bonds with erythritol molecules, and more energy is needed to break the hydrogen bonds, thereby increasing the solidification time of NePCMs. Therefore, in the case of more nanoparticles, it may also lead to longer charging and discharging time. The effect of TEA on the phase change properties of erythritol will be further investigated in our future work.

As we can see from Figure 10f, the T_0 of all NePCMs is higher than pure erythritol of 14.03°C, attributed to adding nanoparticles or the TEA. It is noteworthy that the value of T_0 we got from the 24 charging/discharging cycle test is entirely different from the results obtained from the DSC curves. It is because the quality and size of the sample can affect the supercooling degree severely, and a larger sample is more practical for engineering applications. These results indicate that the supercooling degree of large erythritol is much smaller than that of small erythritol, and the addition of TEA does not significantly change the supercooling degree of erythritol, which can be further proved by the results in Figure 10c.

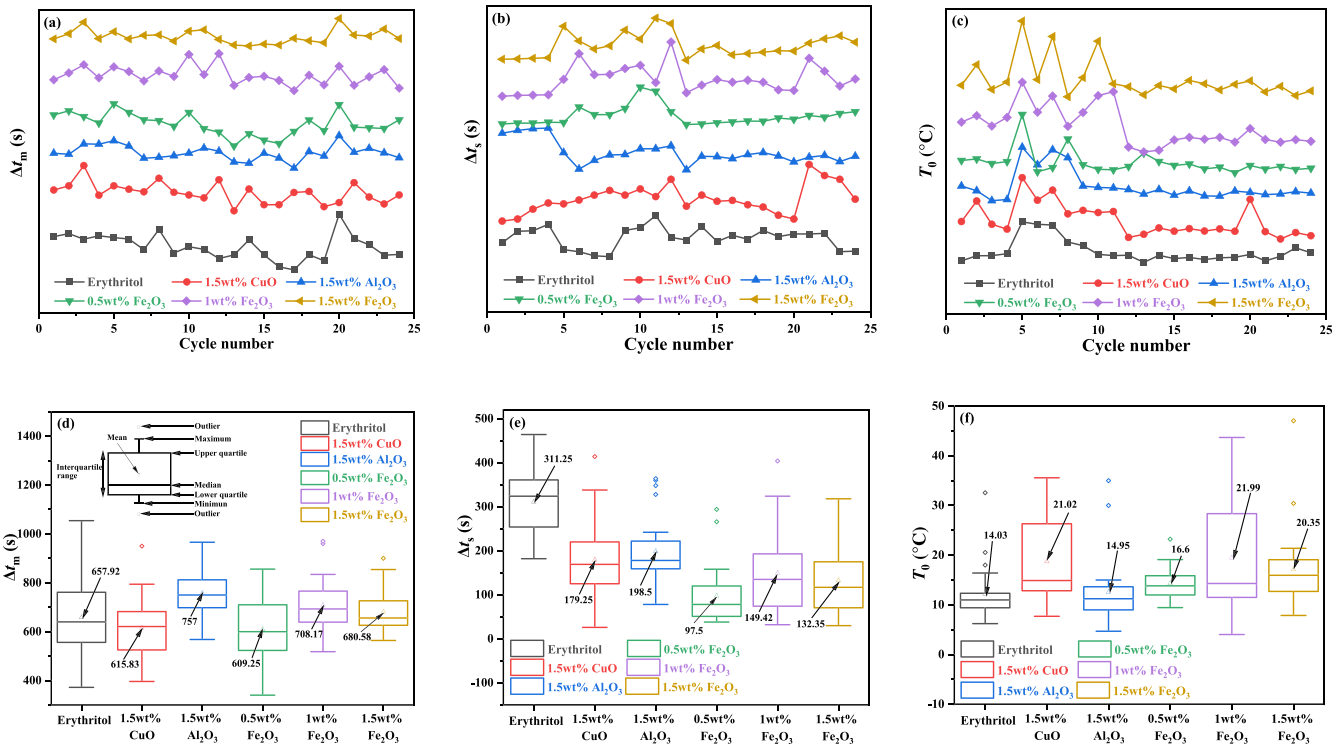

FIGURE 10 Variation of (a) Δt_m, (b) Δt_s, and (c) T_0 with the cycle number and the box chart of (d) Δt_m, (e) Δt_s, and (f) T_0 during the 24 charging/discharging cycles for different NePCMs

19322143, 2022, 2, Downloaded from https://onlinelibrary.wiley.com/doi/10.1002/apj.2754 by Zhejiang University, Wiley Online Library on [12/02/2023]. See the Terms and Conditions (https://onlinelibrary.wiley.com/terms-and-conditions) on Wiley Online Library for rules of use; OA articles are governed by the applicable Creative Commons License

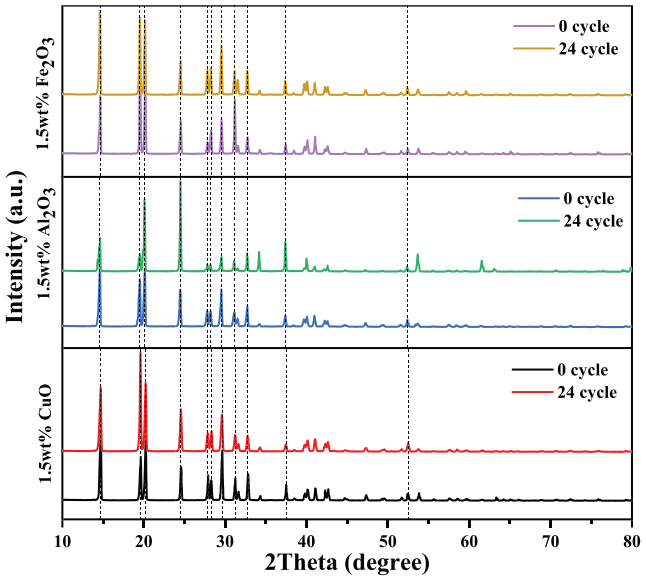

FIGURE 11 XRD patterns of 1.5 wt% CuO, Al_2O_3, and Fe_2O_3 NePCMs before and after the 24 charging/discharging cycle test

3.6 | Cyclic stability of NePCMs

After the charging/discharging cycle test, an XRD test was conducted again by taking a small amount of sample from the center of 1.5 wt% CuO, Al_2O_3, and Fe_2O_3 NePCMs. Figure 11 reveals the XRD patterns of the NePCMs before and after the cycle test. It can be found that, except for the change in the peak intensity, no new absorption peak was observed in the XRD patterns, which indicates that the NePCMs did not undergo chemical changes during the 24 cycle test.

4 | CONCLUSION

The purpose of the article was to compare the effect of three kinds of nanoparticles (CuO, Al_2O_3, and Fe_2O_3) and TEA as heat transfer enhancers and dispersant on the thermal properties of erythritol. According to the results of characterizations and experiments, the sedimentation of nanoparticles in erythritol, chemical stability, thermal conductivity, phase change properties, and charging/discharging cyclic behaviors were researched. Based on the results, the following primary findings can be summarized:

1. The results of XRD before and after the 24 cycle test show that whether in the preparation process or the long period of charging/discharging test, the NePCMs have excellent chemical compatibility and chemical stability.
2. According to the results of thermal conductivity and microstructure of erythritol and NePCMs, the CuO and Fe_2O_3 nanoparticles can enhance heat transfer effectively. Compared with the thermal of 0.671 W/(m·K) for erythritol, it was increased to 0.722 W/(m·K) and 0.761 W/(m·K) of 1.5 wt% CuO and 1.5 wt % Fe_2O_3 NePCMs, respectively. However, the effect of Al_2O_3 nanoparticles was ambiguous, which can be confirmed by the cycle test results.
3. The TEA is a valuable dispersant for three kinds of nanoparticles, especially for CuO and Al_2O_3 nanoparticles. Moreover, based on the results of DSC curves, adding TEA into erythritol significantly increases the melting temperature and heat of fusion of NePCMs, such as the melting temperature and heat of fusion of 1.5 wt% CuO NePCM increased from 110.09°C and 288.9 kJ/kg to 122.52°C and 347.8 kJ/kg after adding TEA, respectively.
4. During the 24 charging/discharging cycle test, the representative charging time, representative discharging time, and supercooling degree of erythritol and NePCMs kept relatively stable, demonstrating the chemical stability again. Compared with pure erythritol, the representative discharging time was reduced by 42.4%, 36.2%, and 57.5% for the 1.5 wt% CuO, Al_2O_3, and Fe_2O_3 NePCMs, respectively. The supercooling degree of NePCMs was close to that of erythritol, which was different from the results obtained from DSC.

The presented experimental results testify that CuO and Fe_2O_3 nanoparticles can effectively enhance heat transfer of erythritol, and the effect of TEA on erythritol will be studied in our future work.

ACKNOWLEDGEMENT

This work is supported by the National Natural Science Foundation of China (no. 52036008).

NOMENCLATURE

Symbols

T_0	supercooling degree (°C)
T_m	melting temperature (°C)
T_p	peak temperature (°C)
T_s	solidification temperature (°C)
T_t	turning temperature (°C)
Δt_m	representation charging time (s)
Δt_s	representation discharging time (s)

ORCID

Hao Zhou https://orcid.org/0000-0001-9779-7703

19322143, 2022, 2, Downloaded from https://onlinelibrary.wiley.com/doi/10.1002/apj.2754 by Zhejiang University, Wiley Online Library on [12/02/2023]. See the Terms and Conditions (https://onlinelibrary.wiley.com/terms-and-conditions) on Wiley Online Library for rules of use; OA articles are governed by the applicable Creative Commons License

REFERENCES

1. Koohi-Fayegh S, Rosen MA. A review of energy storage types, applications and recent developments. *J Storage Mater*. 2020; 27:101047. doi:10.1016/j.est.2019.101047
2. Alhuyi Nazari M, Salem M, Mahariq I, Younes K, Maqableh BB. Utilization of data-driven methods in solar desalination systems: a comprehensive review. *Front Energy Res*. 2021;9. doi:10.3389/fenrg.2021.742615
3. Ibáñez M, Cabeza LF, Solé C, Roca J, Nogués M. Modelization of a water tank including a PCM module. *Appl Therm Eng*. 2006;26(11–12):1328-1333. doi:10.1016/j.applthermaleng.2005.10.022
4. Haillot D, Franquet E, Gibout S, Bédécarrats J-P. Optimization of solar DHW system including PCM media. *Appl Energy*. 2013;109:470-475. doi:10.1016/j.apenergy.2012.09.062
5. Gautam A, Saini RP. A review on sensible heat based packed bed solar thermal energy storage system for low temperature applications. *Sol Energy*. 2020;207:937-956. doi:10.1016/j.solener.2020.07.027
6. Mohan G, Venkataraman MB, Coventry J. Sensible energy storage options for concentrating solar power plants operating above 600 °C. *Renew Sust Energ Rev*. 2019;107:319-337. doi:10.1016/j.rser.2019.01.062
7. Li G. Sensible heat thermal storage energy and exergy performance evaluations. *Renew Sust Energ Rev*. 2016;53:897-923. doi:10.1016/j.rser.2015.09.006
8. Wu S, Yan T, Kuai Z, Pan W. Thermal conductivity enhancement on phase change materials for thermal energy storage: a review. *Energy Storage Mater*. 2020;25:251-295. doi:10.1016/j.ensm.2019.10.010
9. Du K, Calautit J, Wang Z, Wu Y, Liu H. A review of the applications of phase change materials in cooling, heating and power generation in different temperature ranges. *Appl Energy*. 2018;220:242-273. doi:10.1016/j.apenergy.2018.03.005
10. Nazir H, Batool M, Bolivar Osorio FJ, et al. Recent developments in phase change materials for energy storage applications: a review. *Int J Heat Mass Transf*. 2019;129:491-523. doi:10.1016/j.ijheatmasstransfer.2018.09.126
11. Jarimi H, Aydin D, Yanan Z, Ozankaya G, Chen X, Riffat S. Review on the recent progress of thermochemical materials and processes for solar thermal energy storage and industrial waste heat recovery. *Int J Low Carbon Technol*. 2019;14(1):44-69. doi:10.1093/ijlct/cty052
12. Pardo P, Deydier A, Anxionnaz-Minvielle Z, Rougé S, Cabassud M, Cognet P. A review on high temperature thermochemical heat energy storage. *Renew Sust Energ Rev*. 2014;32:591-610. doi:10.1016/j.rser.2013.12.014
13. Sunku Prasad J, Muthukumar P, Desai F, Basu DN, Rahman MM. A critical review of high-temperature reversible thermochemical energy storage systems. *Appl Energy*. 2019;254:113733. doi:10.1016/j.apenergy.2019.113733
14. Zhou H, Lv L, Zhang Y, Ji M, Cen K. Preparation and characterization of a shape-stable xylitol/expanded graphite composite phase change material for thermal energy storage. *Sol Energy Mater Sol Cells*. 2021;230:111244. doi:10.1016/j.solmat.2021.111244
15. Wei G, Wang G, Xu C, et al. Selection principles and thermophysical properties of high temperature phase change materials for thermal energy storage: a review. *Renew Sust Energ Rev*. 2018;81:1771-1786. doi:10.1016/j.rser.2017.05.271
16. Hoshi A, Mills DR, Bittar A, Saitoh TS. Screening of high melting point phase change materials (PCM) in solar thermal concentrating technology based on CLFR. *Sol Energy*. 2005;79(3):332-339. doi:10.1016/j.solener.2004.04.023
17. Yuan M, Ren Y, Xu C, Ye F, Du X. Characterization and stability study of a form-stable erythritol/expanded graphite composite phase change material for thermal energy storage. *Renew Energy*. 2019;136:211-222. doi:10.1016/j.renene.2018.12.107
18. Qureshi ZA, Ali HM, Khushnood S. Recent advances on thermal conductivity enhancement of phase change materials for energy storage system: a review. *Int J Heat Mass Transf*. 2018;127:838-856. doi:10.1016/j.ijheatmasstransfer.2018.08.049
19. Farzanehnia A, Khatibi M, Sardarabadi M, Passandideh-Fard M. Experimental investigation of multiwall carbon nanotube/paraffin based heat sink for electronic device thermal management. *Energy Convers Manag*. 2019;179:314-325. doi:10.1016/j.enconman.2018.10.037
20. Zhichao L, Qiang Z, Gaohui W. Preparation and enhanced heat capacity of nano-titania doped erythritol as phase change material. *Int J Heat Mass Transf*. 2015;80:653-659. doi:10.1016/j.ijheatmasstransfer.2014.09.069
21. Xiao X, Zhang P, Li M. Preparation and thermal characterization of paraffin/metal foam composite phase change material. *Appl Energy*. 2013;112:1357-1366. doi:10.1016/j.apenergy.2013.04.050
22. Esapour M, Hamzehnezhad A, Rabienataj Darzi AA, Jourabian M. Melting and solidification of PCM embedded in porous metal foam in horizontal multi-tube heat storage system. *Energy Convers Manag*. 2018;171:398-410. doi:10.1016/j.enconman.2018.05.086
23. Sardari PT, Giddings D, Grant D, Gillott M, Walker GS. Discharge of a composite metal foam/phase change material to air heat exchanger for a domestic thermal storage unit. *Renew Energy*. 2020;148:987-1001. doi:10.1016/j.renene.2019.10.084
24. Zhao Y, Jin L, Zou B, et al. Expanded graphite–paraffin composite phase change materials: effect of particle size on the composite structure and properties. *Appl Therm Eng*. 2020;171:115015. doi:10.1016/j.applthermaleng.2020.115015
25. Ren Y, Xu C, Yuan M, Ye F, Ju X, Du X. $Ca(NO_3)_2$-$NaNO_3$/expanded graphite composite as a novel shape-stable phase change material for mid- to high-temperature thermal energy storage. *Energy Convers Manag*. 2018;163:50-58. doi:10.1016/j.enconman.2018.02.057
26. Wang Y, Li S, Zhang T, Zhang D, Ji H. Supercooling suppression and thermal behavior improvement of erythritol as phase change material for thermal energy storage. *Sol Energy Mater Sol Cells*. 2017;171:60-71. doi:10.1016/j.solmat.2017.06.027
27. Li JF, Lu W, Zeng YB, Luo ZP. Simultaneous enhancement of latent heat and thermal conductivity of docosane-based phase change material in the presence of spongy graphene. *Sol Energy Mater Sol Cells*. 2014;128:48-51. doi:10.1016/j.solmat.2014.05.018
28. Khodadadi JM, Hosseinizadeh SF. Nanoparticle-enhanced phase change materials (NEPCM) with great potential for improved thermal energy storage. *Int Commun Heat Mass Transfer*. 2007;34(5):534-543. doi:10.1016/j.icheatmasstransfer.2007.02.005

19322143, 2022, 2, Downloaded from https://onlinelibrary.wiley.com/doi/10.1002/apj.2754 by Zhejiang University, Wiley Online Library on [12/02/2023]. See the Terms and Conditions (https://onlinelibrary.wiley.com/terms-and-conditions) on Wiley Online Library for rules of use; OA articles are governed by the applicable Creative Commons License

29. Keblinski P, Eastman JA, Cahill DG. Nanofluids for thermal transport. *Mater Today*. 2005;8(6):36-44. doi:10.1016/s1369-7021(05)70936-6
30. Li L, Zhang Y, Ma H, Yang M. Molecular dynamics simulation of effect of liquid layering around the nanoparticle on the enhanced thermal conductivity of nanofluids. *J Nanopart Res*. 2009;12(3):811-821. doi:10.1007/s11051-009-9728-5
31. Rashidi MM, Nazari MA, Mahariq I, et al. Thermophysical properties of hybrid nanofluids and the proposed models: an updated comprehensive study. *Nanomaterials*. 2021;11(11). doi:10.3390/nano11113084
32. Xu B, Li Z. Paraffin/diatomite/multi-wall carbon nanotubes composite phase change material tailor-made for thermal energy storage cement-based composites. *Energy*. 2014;72:371-380. doi:10.1016/j.energy.2014.05.049
33. Srinivasan S, Diallo MS, Saha SK, Abass OA, Sharma A, Balasubramanian G. Effect of temperature and graphite particle fillers on thermal conductivity and viscosity of phase change material *n*-eicosane. *Int J Heat Mass Transf*. 2017;114:318-323. doi:10.1016/j.ijheatmasstransfer.2017.06.081
34. Zhang Q, Luo Z, Guo Q, Wu G. Preparation and thermal properties of short carbon fibers/erythritol phase change materials. *Energy Convers Manag*. 2017;136:220-228. doi:10.1016/j.enconman.2017.01.023
35. Al Ghossein RM, Hossain MS, Khodadadi JM. Experimental determination of temperature-dependent thermal conductivity of solid eicosane-based silver nanostructure-enhanced phase change materials for thermal energy storage. *Int J Heat Mass Transfer*. 2017;107:697-711. doi:10.1016/j.ijheatmasstransfer.2016.11.059
36. Parameshwaran R, Jayavel R, Kalaiselvam S. Study on thermal properties of organic ester phase-change material embedded with silver nanoparticles. *J Therm Anal Calorim*. 2013;114(2):845-858. doi:10.1007/s10973-013-3064-9
37. Suresh Kumar KR, Dinesh R, Ameelia Roseline A, Kalaiselvam S. Performance analysis of heat pipe aided NEPCM heat sink for transient electronic cooling. *Microelectron Reliab*. 2017;73:1-13. doi:10.1016/j.microrel.2017.04.006
38. Colla L, Fedele L, Mancin S, Danza L, Manca O. Nano-PCMs for enhanced energy storage and passive cooling applications. *Appl Therm Eng*. 2017;110:584-589. doi:10.1016/j.applthermaleng.2016.03.161
39. Şahan N, Fois M, Paksoy H. Improving thermal conductivity phase change materials—a study of paraffin nanomagnetite composites. *Sol Energy Mater Sol Cells*. 2015;137:61-67. doi:10.1016/j.solmat.2015.01.027
40. Parameshwaran R, Dhamodharan P, Kalaiselvam S. Study on thermal storage properties of hybrid nanocomposite-dibasic ester as phase change material. *Thermochim Acta*. 2013;573:106-120. doi:10.1016/j.tca.2013.08.028
41. Parameshwaran R, Deepak K, Saravanan R, Kalaiselvam S. Preparation, thermal and rheological properties of hybrid nanocomposite phase change material for thermal energy storage. *Appl Energy*. 2014;115:320-330. doi:10.1016/j.apenergy.2013.11.029
42. Harikrishnan S, Deenadhayalan M, Kalaiselvam S. Experimental investigation of solidification and melting characteristics of composite PCMs for building heating application. *Energy Convers Manag*. 2014;86:864-872. doi:10.1016/j.enconman.2014.06.042
43. Sharma S, Micheli L, Chang W, Tahir AA, Reddy KS, Mallick TK. Nano-enhanced phase change material for thermal management of BICPV. *Appl Energy*. 2017;208:719-733. doi:10.1016/j.apenergy.2017.09.076
44. Cui W, Yuan Y, Sun L, Cao X, Yang X. Experimental studies on the supercooling and melting/freezing characteristics of nano-copper/sodium acetate trihydrate composite phase change materials. *Renew Energy*. 2016;99:1029-1037. doi:10.1016/j.renene.2016.08.001
45. Venkitaraj KP, Suresh S, Praveen B, Venugopal A, Nair SC. Pentaerythritol with alumina nano additives for thermal energy storage applications. *J Storage Mater*. 2017;13:359-377. doi:10.1016/j.est.2017.08.002
46. Alhuyi Nazari M, Maleki A, Assad MEH, et al. A review of nanomaterial incorporated phase change materials for solar thermal energy storage. *Sol Energy*. 2021;228:725-743. doi:10.1016/j.solener.2021.08.051
47. El Haj Assad M, Alhuyi Nazari M. Chapter 3—heat exchangers and nanofluids. In M.E.H. Assad, M.A. Rosen (Eds.), *Design and Performance Optimization of Renewable Energy Systems*. Academic Press; 2021:33-42. doi:10.1016/B978-0-12-821602-6.00003-1
48. Witharana S, Palabiyik I, Musina Z, Ding Y. Stability of glycol nanofluids—the theory and experiment. *Powder Technol*. 2013;239:72-77. doi:10.1016/j.powtec.2013.01.039
49. Farrokhi-rad M, Ghorbani M. Stability of titania nano-particles in different alcohols. *Ceram Int*. 2012;38(5):3893-3900. doi:10.1016/j.ceramint.2012.01.041
50. Shao X-F, Wang C, Yang Y-J, et al. Screening of sugar alcohols and their binary eutectic mixtures as phase change materials for low-to-medium temperature latent heat storage. (I): non-isothermal melting and crystallization behaviors. *Energy*. 2018;160:1078-1090. doi:10.1016/j.energy.2018.07.081
51. Karthik M, Faik A, Blanco-Rodríguez P, Rodríguez-Aseguinolaza J, D'Aguanno B. Preparation of erythritol–graphite foam phase change composite with enhanced thermal conductivity for thermal energy storage applications. *Carbon*. 2015;94:266-276. doi:10.1016/j.carbon.2015.06.075
52. Huang Z, Gao X, Xu T, Fang Y, Zhang Z. Thermal property measurement and heat storage analysis of $LiNO_3$/KCl–expanded graphite composite phase change material. *Appl Energy*. 2014;115:265-271. doi:10.1016/j.apenergy.2013.11.019
53. Massart DL, Smeyersverbeke AJ, Axc A & Karin SB Practical data handling visual presentation of data by means of box plots; 2010.

How to cite this article: Zhou H, Lv L, Ji M, Zhang Y, Cheng F, Cen K. Experimental study of metal-oxide nanoparticles on the thermal properties of erythritol for thermal energy storage. *Asia-Pac J Chem Eng*. 2022;17(2):e2754. doi:10.1002/apj.2754

19322143, 2022, 2, Downloaded from https://onlinelibrary.wiley.com/doi/10.1002/apj.2754 by Zhejiang University, Wiley Online Library on [12/02/2023]. See the Terms and Conditions (https://onlinelibrary.wiley.com/terms-and-conditions) on Wiley Online Library for rules of use; OA articles are governed by the applicable Creative Commons License